ICF1008870R

FRACTURE STRENGTH OF CERAMIC NOZZLE BLADES UNDER THERMAL SHOCK CONDITIONS

Takao Mikami [1], Koichiro Tagashira [2] and Masakazu Obata [3]

[1] Ishikawajima Inspection & Instrumentation Co., Ltd., Yokohama, JAPAN
[2] Ishikawajima-Harima Heavy Industries Co., Ltd., Tokyo, JAPAN
[3] Kanazawa Institute of Technology, Ishikawa, JAPAN

ABSTRACT

The fracture strength of ceramic turbine nozzle blades is evaluated under instantaneous thermal shock working conditions by a newly developed high-temperature thermal cycle cascade tunnel. The facility was designed to be produced an unsteady thermal stress more than 400MPa for ceramic blades and to confirm the fracture strength. The tunnel operates at a constant speed, with heated gas and ambient temperature air, and has the capability to perform thermal fatigue tests. The objective models are SiC and Si_3N_4 blades with a chord length of 33.6 mm and an aspect ratio of 1.05. The heating and cooling conditions of the test blade were confirmed with steady and transient measurements in the hot gas of 1,400 ºC and ambient cooling air. The measurements include surface temperature distributions on the both sides of the blade. The thermal stress distribution of the test blades was predicted by a finite element method under experimental boundary conditions. Typical results of the transient analysis for the test blades are presented and it is shown that the maximum thermal stress occurs at the leading-edge region of the test blades. The two SiC test blades were fractured at a maximum stress range of 550MPa, but any Si_3N_4 blade was not fractured up to 630MPa. A typical fracture mode of ceramic turbine nozzle blades under instantaneous thermal shock conditions is observed and the fracture mode is presented.

KEYWORDS

Thermal shock, Ceramics, nozzle, Fracture probability, Ceramic gas turbine

INTRODUCTION

Gas turbines have attractive characteristics such as low environmental pollution, fuel versatility and high specific power. An increase of the turbine inlet temperature (TIT) enables a significant improvement in the thermal efficiency of a gas turbine. Using metallic materials, further increase in TIT will not be expected without additional cooling air. One of the most effective means to solve this problem is the application of ceramics to gas turbine components. The application of ceramics to the hot section components enables a significant increase of TIT and the reduction of heat losses through the elimination of blade and nozzle cooling, resulting in improved thermal efficiency and fuel savings. The ceramic gas turbines are, therefore, attractive in terms of the conservation of energy resources and the protection of the environment [1,2].

In order to apply ceramic turbine blades to a gas turbine, we have to evaluate their resistance to thermal shock. Especially turbine nozzles are directly exposed to the high-temperature gas from a combustor and they will meet a high thermal shock in case of gas turbine trip and stop operating conditions.

For this purpose, we developed a high-temperature thermal cycle cascade tunnel to simulate the actual gas

turbine operating conditions and silicon carbide (SiC) and silicon nitride (Si_3N_4) nozzle blades were evaluated. This paper describes the developed apparatus and thermal stress evaluation procedures and test results.

THERMAL CYCLE CASCADE TUNNEL AND TEST NOZZLES

To simulate the actual operating condition of gas turbines, we adopted air and helium flows to a rapid cooling system. The apparatus was designed to enable a cyclic thermal shock testing and consists of a high-temperature gas generator (over 1,400℃), a heating and cooling block of ceramic turbine nozzles, a high-speed traverse unit of the nozzles, a control system and a data acquisition system. The main schematic of the apparatus is shown in Figure 1 in which four nozzles are arranged in a retainer block made of fire- brick as shown in Figure 2.

The block is heated up to a required temperature and then the block is rapidly traversed to the cooling air side at a constant speed. An instantaneous thermal shock test is thus completed. In case of cyclic thermal shock testing, following the above procedure, the block is traversed to the heating side contrary and the procedure is repeated. Considering the uniformity of the flow and temperature distribution, two inside nozzles among four nozzles are evaluated in the tests.

After the nozzles were heated up to 1,400℃, they were cooled by the cooling air. The velocity of the cooling air was increased step by step. The thermal stress induced in Si_3N_4 nozzle is lower than that of SiC because of the difference of the material properties. In case of the Si_3N_4 nozzles helium gas was also used for the cooling in order to increase the thermal stress.

Unsteady temperature distributions of the nozzles during the thermal shock test were monitored by scanning type and fiber type pyrometers.

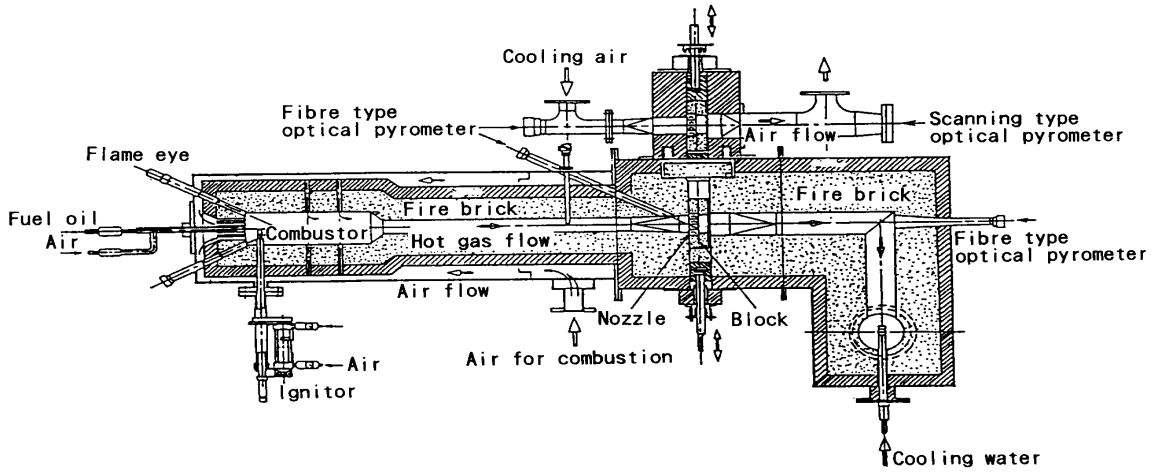

Figure 1: Thermal shock testing facility for turbine nozzle

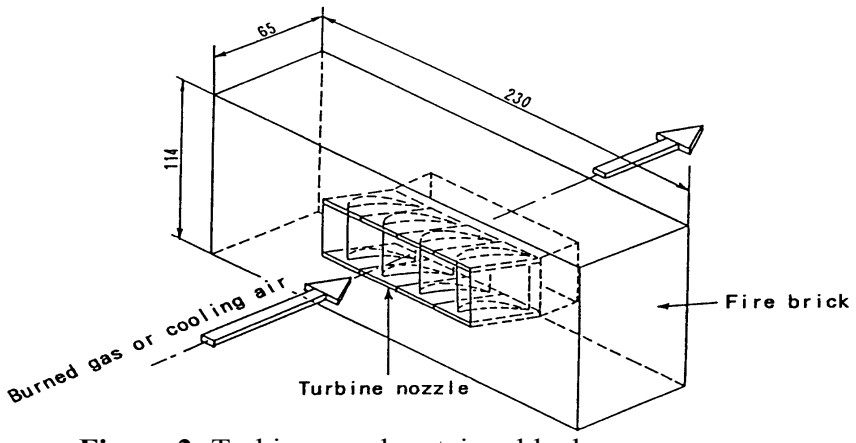

Figure 2: Turbine nozzle retainer block

The configuration of ceramic test nozzles is shown in Figure 3. Two types (Model A and Model B) were designed and were not twisted in considering the easiness of fabrication and analysis.

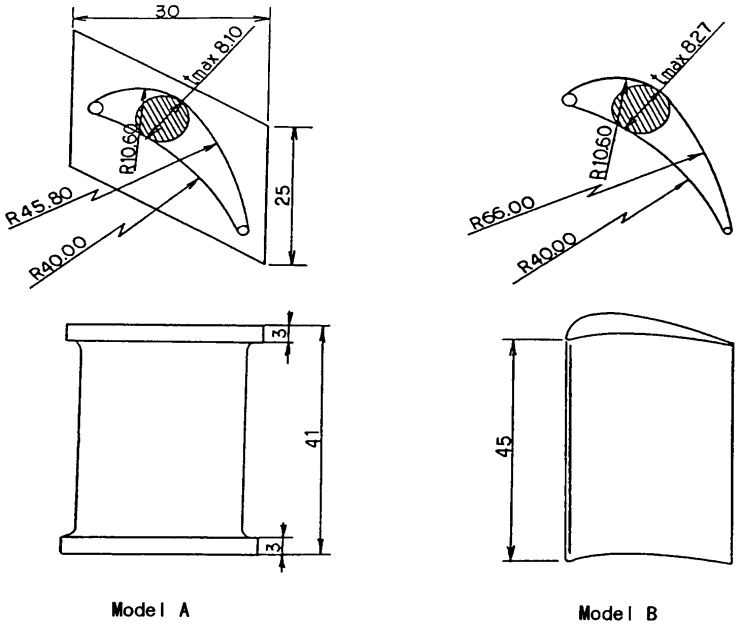

Figure 3: Configurations of turbine nozzle models

UNSTEADY THERMAL STRESS ANALYSIS

Figure 4 shows the flow chart of the test blade design and unsteady stress analysis procedure.
First heat transfer coefficients on the blade surfaces were calculated by a boundary layer approximation method using the specified velocity distribution on the blade surface.
Next, the unsteady temperature and stress distributions of the nozzle are analyzed by the MSC/NASTRAN program.
In the present study, the target strength of the material at 1,400℃was over 400MPa.

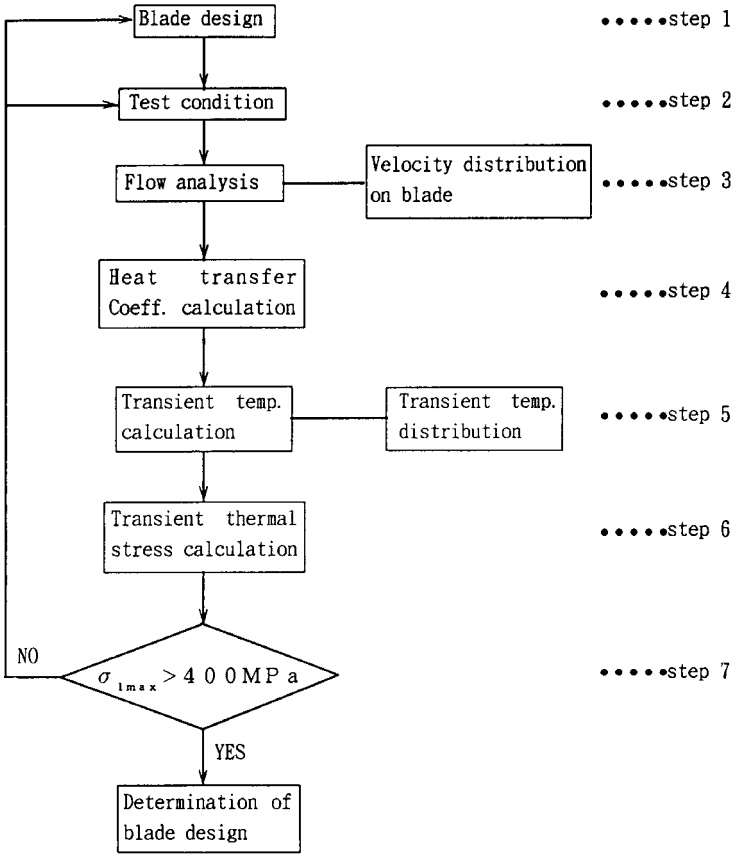

Figure 4: Flow chart of the test blade design and unsteady stress analysis procedure

TEST RESULTS AND DISCUSSION

Results for Model A

Test results for ten pieces of SiC nozzles is shown in Table 1. Any nozzles were not fractured though the cooling air velocity was increased up to 164m/s (630MPa in terms of stress). An analytical result of the thermal stress for one half model is shown in Figure 5(a). The maximum stress occurs at the leading edge. Figure 6 shows a transient thermal stresses with a change of air velocities. As for the leading edge, the stress increases rapidly as soon as cooling starts and after 1 to 2 seconds it reaches a peak value and then it decreases. On the other hand, as for the trailing edge the stress increases gradually and after 5 seconds it reaches a peak value and then it gradually decreases.

TABLE 1
TEST RESULTS OF MODEL A (SiC)

Model NO.	Cooling air		Initial temperature (℃)			Temperature at max. thermal stress (℃)			Max. thermal stress (MPa)
	Flow rate Q (m^3/h)	Velocity U (m/s)	Max. Camber	Trailing Edge	Leading Edge	Max. Camber	Trailing Edge	Leading Edge	
1,2	1,000	106	1,350	1,190	-	1,290	1,140	-	530
3,4	1,015	107	1,380	1,210	765	1,300	1,170	680	530
5	1,030	164	1,370	1,160	-	1,300	1,110	-	630
6	900	144	1,350	1,170	-	1,310	1,100	-	600
7	1,027	164	1,360	1,130	755	1,310	1,090	660	630
8,9	1,027	106	1,380	1,190	-	1,300	1,140	-	530
10	1,030	164	1,370	1,140	780	1,310	1,100	680	630

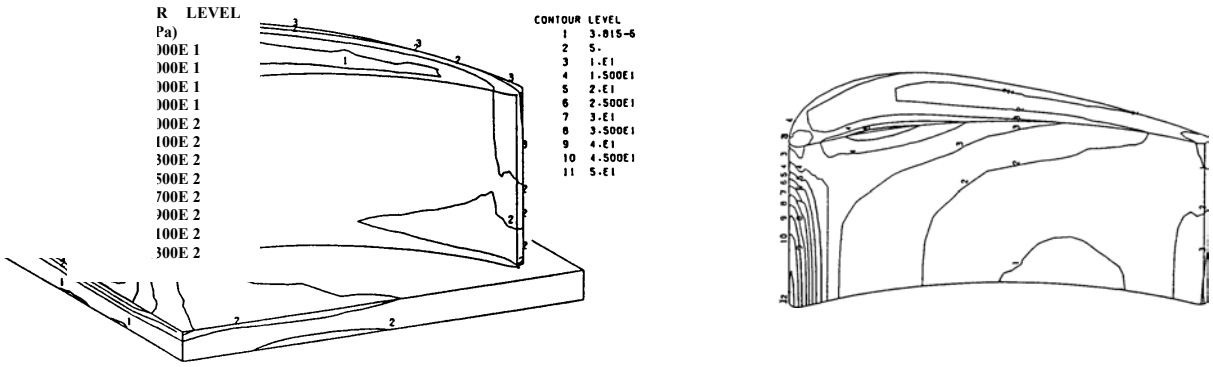

Model A (SiC, U=100m/s with air after two seconds) Model B (Si_3N_4, U=100m/s with air after two seconds)

Figure 5: Thermal stress of Model A and Model B

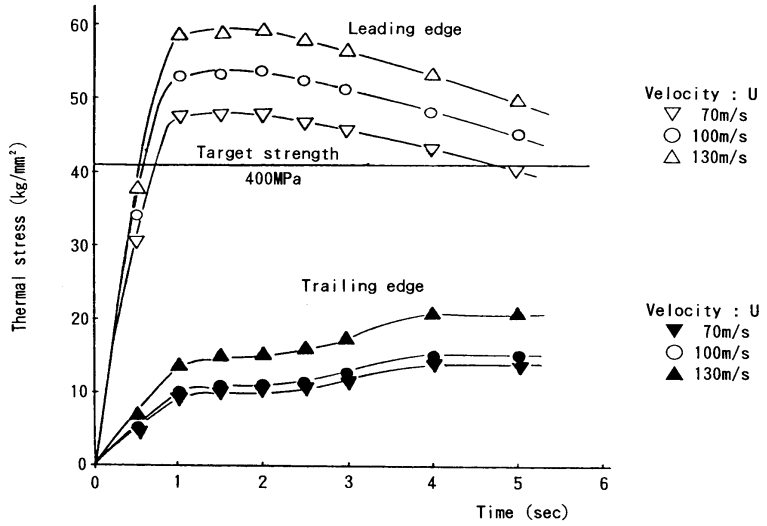

Figure 6: Transient thermal stress of Model A

Results for Model B

Test results for seventeen pieces of SiC nozzles and eight pieces of Si_3N_4 nozzles are shown in Table 2 and Table 3 respectively. As shown in Table 2, two SiC nozzles were fractured at 550MPa and 530MPa.
The fracture mode is shown in Figure 7.
As for the Si_3N_4 nozzles, they were not fractured though the velocity of helium gas was increased up to 160m/s (470MPa in terms of stress). An analytical result of the thermal stress for one half model is shown in Figure 5(b).

TABLE 2
TEST RESULTS OF MODEL B (SiC)

Model NO.	Cooling air		Initial temperature (℃)			Temperature at max. thermal stress (℃)			Max. thermal stress (MPa)
	Flow rate Q (m^3/h)	Velocity U (m/s)	Max. Camber	Trailing Edge	Leading Edge	Max. Camber	Trailing Edge	Leading Edge	
1,2	1,022	109	1,340	1,100	-	1,290	1,070	-	510
3,4	1,027	109	1,380	1,160	-	1,290	1,100	-	510
5	854	130	1,370	1,180	-	1,300	1,120	-	**550(Frac.)**
6	1,000	160	1,360	1,170	780	1,310	1,100	750	600
7	1,039	166	1,380	1,110	-	1,300	1,090	-	630
8	1,000	160	1,385	1,120	800	1,310	1,090	780	530
9	903	144	1,360	1,180	800	1,310	1,025	720	570
10,11	1,010	107	1,380	1,250	-	1,320	1,160	-	510
12,13	1,027	109	1,370	1,200	-	1,300	1,130	-	510
14	700	112	1,370	1,210	-	1,340	1,150	-	**530(Frac.)**
15	1,030	164	1,370	1,200	770	1,320	1,100	750	590
16	840	134	1,340	1,210		1,280	1,170		550
17	1,027	164	1,370	1,150	780	1,330	1,080	760	590

TABLE 3
TEST RESULTS OF MODEL B (Si_3N_4)

Model NO.	Cooling air		Initial temperature (℃)			Temperature at max. thermal stress (℃)			Max. thermal stress (MPa)
	Flow rate Q (m^3/h)	Velocity U (m/s)	Max. Camber	Trailing Edge	Leading Edge	Max. Camber	Trailing Edge	Leading Edge	
1	906	145	1,360	1,160	-	1,290	1,110	-	245
2	900	144	1,380	1,120	-	1,310	1,070	-	245
3	1,040	168	1,370	1,140	-	1,330	1,090	-	265
*4	360	80	1,400	1,355	-	1,340	1,190	-	400
*5	432	96	1,385	1,280	-	1,280	1,130	-	420
*6	576	128	1,385	1,280	-	1,130	875	-	450
*7	720	160	1,370	1,280	-	1,145	920	-	470
*8	617	137	1,355	1,280	-	1,205	995	-	460

*cooling by helium gas

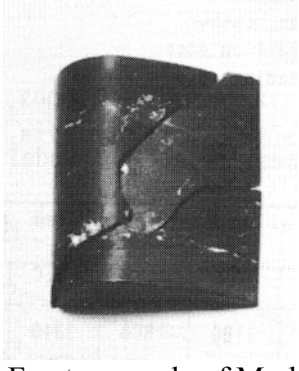

Figure 7: Fracture mode of Model B (SiC)

Fracture Probability

Figure 8 shows the time history of thermal stresses (σ) and the effective volume (Ve), fracture probability (P_f) for a Model A (SiC). It is shown that because of the smaller effective volume, the fracture probability of the nozzle is lower than approximately 10 % and this is considered to be similar to that of other test pieces. It is therefore considered that any Model A were not fractured in the thermal shock tests.

On the other hand, the stress level of Model B is lower than that of Model A, but two nozzles were fractured in the tests. It is because the cause of fracture depended on the difference of fracture probability between Model A and Model B, which gave a higher value. This high fracture probability in Model B resulted from the difference of stress gradient between the two Models as shown in Figure 5(a) and (b).

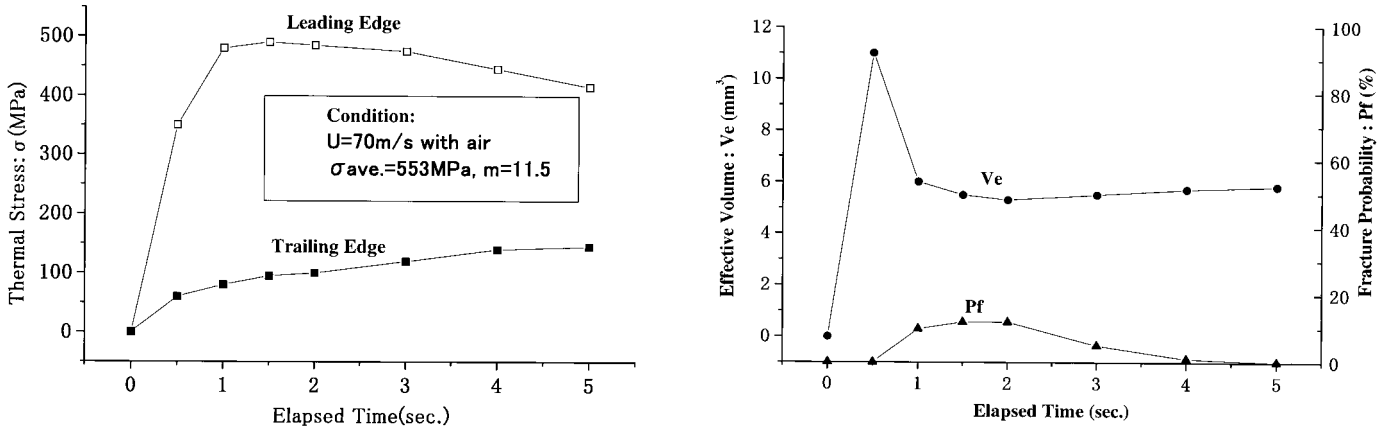

Figure 8: Time history of σ and Ve, P_f of Model A

CONCULUSIONS

A high-temperature thermal shock testing facility and fracture evaluating procedures for ceramic blades were developed. The typical fracture characteristics of ceramic turbine nozzle blade under instantaneous thermal shock condition were clarified and the fracture mode was presented.

ACKNOWLEDGEMENTS

This work was conducted under a contract from the Agency of Industrial Science and Technology of the Ministry of International Trade and Industry (AIST/MITI). We appreciate their advice and support.

REFERENCES

1. Mikami, T. et al (1996). Status of the Development of the CGT301, a 300 KW Class Ceramic Gas Turbine, ASME 96-GT-252, ASME TURBO EXPO'96, Birmingham, UK
2. Mikami, T. et al (1998). Application of Ceramics to the CGT301, a 300 KW Class Ceramic Gas Turbine, CIMTEC 98, Florence, Italy